

# Coordination properties of the ACE inhibitor captopril towards $\text{Me}_2\text{Sn(IV)}^{2+}$ in aqueous solution, and biological aspects of some dialkyltin(IV) derivatives of this ligand

Hajnalka Jankovics<sup>a</sup>, László Nagy<sup>b,\*</sup>, Zoltán Kele<sup>c</sup>, Claudio Pettinari<sup>d</sup>,  
Paolo D'Agati<sup>e</sup>, Caterina Mansueto<sup>e</sup>, Claudia Pellerito<sup>f</sup>, Lorenzo Pellerito<sup>f</sup>

<sup>a</sup> Biocoordination Research Group of Hungarian Academy of Sciences, Department of Inorganic and Analytical Chemistry, University of Szeged, H-6701 Szeged, Hungary

<sup>b</sup> Department of Inorganic and Analytical Chemistry, University of Szeged, H-6701 Szeged, P.O. Box 440, Hungary

<sup>c</sup> Medical Chemistry Department, University of Szeged, H-6701 Szeged, Hungary

<sup>d</sup> Department of Chemistry, University of Camerino, 62032 Camerino, via S. Agostino 1, Italy

<sup>e</sup> Department of Animal Biology, University of Palermo, Via Archirafi 18, 90123 Palermo, Italy

<sup>f</sup> Department of Inorganic and Analytical Chemistry, University of Palermo, Parco d'Orleans, Viale delle Scienze, 90128 Palermo, Italy

Received 30 September 2002; received in revised form 6 January 2003; accepted 6 January 2003

## Abstract

The coordination of  $\text{Me}_2\text{Sn(IV)}^{2+}$  ( $=\text{M}$ ) to captopril  $\{N-[(S)-3\text{-mercapto-2-methylpropionyl}]-L\text{-proline, } =\text{H}_2(\text{cap}), \text{H}_2\text{L}\}$  in aqueous solution was studied by means of potentiometric titration, electro spray mass spectrometry,  $^1\text{H-NMR}$  spectroscopy and Mössbauer spectroscopy in the pH range 2–11 ( $I = 0.1 \text{ mol dm}^{-3} \text{ NaClO}_4$ , 298 K). The results obtained with these methods proved that only monomeric complexes are formed in solution. In the acidic pH range, species with a metal-to-ligand ratio of 1:1 exist. The neutral complex ML, similarly to the complex  $\text{Me}_2\text{Sn}(\text{cap})$  crystallized in the same pH range, adopts a *tbp* structure with *eq*  $-\text{S}^-$  and *ax*  $-\text{COO}^-$ , while, instead of the coordination of the amide  $-\text{C}=\text{O}$ , observed in the solid state, the other *ax* position is occupied by a  $\text{H}_2\text{O}$  molecule. With increasing pH, in the neutral and weakly basic pH range the complexes  $\text{MLH}_{-1}$  and  $\text{ML}_2$  are formed, in which the  $-\text{COO}^-$  group is displaced from the coordination sphere by an  $\text{OH}^-$  and an  $\text{S}^-$  of another ligand, respectively. Biological activity tests on  $\text{Me}_2\text{Sn}(\text{cap})$  and three further  $\text{R}_2\text{Sn(IV)}$  captopril complexes showed that *n*- $\text{Bu}_2\text{Sn}(\text{cap})$  and *t*- $\text{Bu}_2\text{Sn}(\text{cap})$  exert toxic activity towards the embryos of *Ciona intestinalis*, while the ligand itself does not affect the development of the embryos to any significant extent;  $\text{Me}_2\text{Sn}(\text{cap})$  and  $\text{Et}_2\text{Sn}(\text{cap})$  produced normal swimming larvae.

© 2003 Elsevier Science B.V. All rights reserved.

**Keywords:** Organotin compounds; pH-metric titration; Mass spectrometry; Mössbauer; NMR studies; Cytotoxicity

## 1. Introduction

Captopril is used therapeutically as an antihypertensive agent. It acts as a potent and specific inhibitor of the zinc-containing angiotensin converting enzyme (ACE) [1] (Fig. 1).

On the other hand, the side-effects that can arise during captopril treatment [2] may well be caused by the interactions of captopril with other metal ions present in the plasma [3]. To gain a deeper insight into the

mechanism of the inhibition and side-effects of captopril, equilibrium and structural studies were earlier performed with several metal ions [4–7]. Reports have also appeared on the use of transition metal ions for the indirect quantitative spectrophotometric determination of captopril in pharmaceutical formulations [8].

Captopril is a pseudo-cysteinyl-proline dipeptide. In biological media, the thiol groups of cysteine residues are known to be among the main binding sites for organotin(IV) compounds, yielding products with Sn–S bonds [9,10]. Moreover,  $\text{R}_2\text{Sn(IV)}$  cysteinates have been found to be active against murine leukaemia P-388 [11]. Organotin(IV) complexes of D- and L-penicillamine

\* Corresponding author.

E-mail address: [laci@chem.u-szeged.hu](mailto:laci@chem.u-szeged.hu) (L. Nagy).

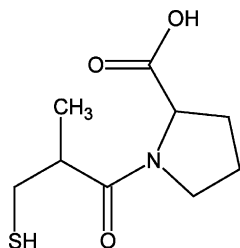


Fig. 1. Molecular structure of captopril.

have been tested to examine the role of chirality on the antitumour effect; it was found to be irrelevant [12]. The interactions between organotin(IV) compounds and reduced glutathione have also been investigated in aqueous solution [13,14]. The interactions of cysteine and two protected derivatives towards  $\text{Et}_2\text{Sn(IV)}^{2+}$  confirmed that the thiolate group has a strong ability to bind organotin(IV) cations [15].

The first study on the interactions of captopril with organometallic compounds was performed recently [16]. The structures of solid  $\text{R}_2\text{Sn(IV)}$  complexes were reported and compared with each other and with those of zinc complexes of this ligand. Additionally, the first X-ray structure of a captopril complex [ $\text{Me}_2\text{Sn}(\text{cap})$ ] was demonstrated.

To add to the results on solid  $\text{R}_2\text{Sn(IV)}$  complexes [16], we have now extended our studies to the interactions of captopril with  $\text{Me}_2\text{Sn(IV)}^{2+}$  in aqueous solution in the pH range 2–11. In this work, the equilibrium behaviour and possible structures of the complexes formed under these conditions will be discussed on the basis of pH-metric titrations, and electrospray mass spectrometric, and  $^1\text{H-NMR}$  and Mössbauer spectroscopic results. Moreover, to evaluate the possible cytotoxicity of the neutral complex  $\text{Me}_2\text{Sn}(\text{cap})$  and related  $\text{R}_2\text{Sn(IV)}$  derivatives of captopril synthesized earlier, the development of *Ciona intestinalis* embryos after treatment with these complexes was analysed.

## 2. Experimental

### 2.1. Materials

$\text{Me}_2\text{SnCl}_2$  (Fluka) solution was standardized potentiometrically by pH-metric titration with NaOH (Fluka) solution. Captopril was a Sigma product of analytical purity and was used without further purification. One portion of the ligand was presented by EGIS Pharmaceutical Company, Hungary.

### 2.2. pH-metric measurements

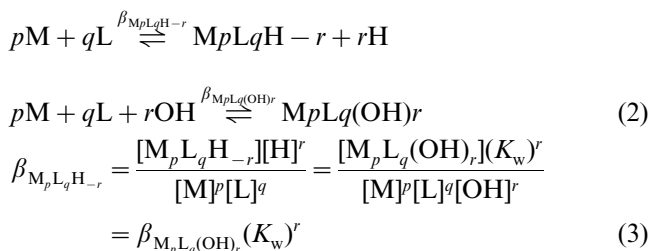
Coordination equilibria were investigated by potentiometric titration in aqueous solution. The ionic

strength was adjusted to  $0.1 \text{ mol dm}^{-3}$  with  $\text{NaClO}_4$ , and the cell was thermostated to  $298 \pm 0.1 \text{ K}$ . The electrode (Orion Ross 8102) was calibrated by the titration of  $\text{HClO}_4$  with an NaOH solution of known composition. The electrode potential was recorded with an Orion 710A precision digital pH-meter in a full automatic titration set. The measured e.m.f. values ( $E$ ), were converted to hydrogen ion concentrations by using the modified Nernst equation [17] (Eq. (1)):

$$E = E_0 + K \log[\text{H}^+] + J_{\text{H}}[\text{H}^+] + \frac{J_{\text{OH}}K_{\text{w}}}{[\text{H}^+]} \quad (1)$$

where  $J_{\text{H}}$  and  $J_{\text{OH}}$  are fitting parameters in acidic and alkaline media for the correction of experimental errors, mainly due to the liquid junction and to the alkaline and acidic errors of the glass electrode;  $K_{\text{w}}$  is the autoprotolysis constant of water:  $10^{-13.75}$  at 298 K [18]. The parameters were calculated by a non-linear least squares method.

The species formed in the systems studied were characterized by the general equilibrium processes Eq. (2), while the formation constants for these generalized species are given by Eq. (3):



(Charges are omitted for simplicity; M denotes  $\text{Me}_2\text{Sn(IV)}^{2+}$  and L the ligand molecule deprotonated on its carboxyl and thiol groups. The charge on L is  $-2$ .)

The equilibrium constants were all determined from three independent titrations (80–100 points for each titration), using an  $\text{Me}_2\text{Sn(IV)}$ -to-ligand ratios of from 2:1 to 1:5. Solubilities were determined by preliminary measurements. In the  $\text{Me}_2\text{Sn(IV)}$ -captopril system the  $\text{Me}_2\text{Sn(IV)}$  concentration ranged from  $1.25 \times 10^{-3}$  to  $5 \times 10^{-3} \text{ mol dm}^{-3}$ . The experimental data were evaluated by the computer program PSEQUAD [19].

### 2.3. Mass spectrometry

Mass spectrometric measurements were obtained on a Finnigan TSQ-7000 triple quadrupole mass spectrometer (Finnigan-MAT, San Jose, CA) equipped with a Finnigan ESI source. The instrument was scanned both positive and negative ion mode in a mass range of 10–1500 with a scan time of 1.5 s. Spectra were produced via infusion of sample with a Harvard Apparatus 22 syringe pump (South Natick, MA) driving a 250  $\mu\text{l}$  glass

syringe with a stainless steel needle attached to 50  $\mu\text{m}$  i.d. fused silica capillary tubing via a Teflon coupling at the syringe needle. The electrospray needle is adjusted to 4.5 kV and  $\text{N}_2$  was used as a nebulizer gas. The computer program used for simulation of theoretical isotope distributions is included in the ICIS 8.3 package.

#### 2.4. NMR measurements

$^1\text{H}$ -NMR spectra were recorded on a VXR-300 Varian spectrometer (University of Camerino, Italy) operating at room temperature, 300 MHz, with 16–32K data points. A suitable signal-to-noise ratio was achieved after the collection of 16–64 transients. During the recycling delay, the water resonance was suppressed. The proton chemical shifts,  $\delta$ , were measured with respect to  $(\text{CH}_3)_2\text{Si}(\text{CD}_2)_2\text{ONa}$  as reference. Measurements were generally made in  $\text{H}_2\text{O}-\text{D}_2\text{O}$  (5:1). Samples were prepared as 0.01 mol  $\text{dm}^{-3}$  solutions containing  $\text{Me}_2\text{Sn}(\text{IV})^{2+}$  and the ligand in a metal-to-ligand ratio of 1:1.  $^{13}\text{C}$ - and  $^{119}\text{Sn}$ -NMR spectra were recorded on a Bruker Avance DRX-500 spectrometer (University of Szeged, Hungary) at 125.8 and 111.9 Hz, respectively.

#### 2.5. Mössbauer measurements

The  $^{119}\text{Sn}$  Mössbauer spectra of quick-frozen solutions were obtained with a  $\text{Ca}^{119}\text{SnO}_3$  (10 mCi, Radiochemical Centre, Amersham, UK) source at room temperature. The absorber samples of the  $\text{Me}_2\text{Sn}(\text{IV})^{2+}$  derivatives investigated, in concentrations ranging from  $5 \times 10^{-3}$  to  $110^{-2}$  mol  $\text{dm}^{-3}$ , were contained in cylindrical polythene sample holders ( $\sim 1$  ml, 1  $\text{cm}^2$  cross-section, corresponding to 0.025–0.050 mg  $^{119}\text{Sn}$   $\text{cm}^{-2}$ ) and maintained at liquid nitrogen temperature,  $77.3 \pm 0.1$  K. The source motion was effected by a Wissenschaftliche Elektronik GMBH apparatus (Germany). Velocity calibration was carried out with an enriched iron foil spectrum ( $^{57}\text{Fe} = 99.99\%$ , thickness 0.06 mm, Dupont, MA) at room temperature, using a  $^{57}\text{Co}$  source (10 mCi, Dupont, MA) in a palladium matrix, while the zero point of the Doppler velocity was determined at room temperature via the absorption spectrum of natural  $\text{BaSnO}_3$  containing 0.5 mg  $\text{cm}^{-2}$  of  $^{119}\text{Sn}$ .  $5 \times 10^5$  counts were collected for each velocity point and the obtained data were refined with appropriate software to obtain the Mössbauer parameter isomer shift,  $\delta$  ( $\text{mm s}^{-1}$ ), nuclear quadrupole splitting,  $|\Delta|$  ( $\text{mm s}^{-1}$ ), and the width at half-height of the resonant peaks,  $\Gamma$  ( $\text{mm s}^{-1}$ ).

Comparison of the experimental  $|\Delta|$  values with those calculated on the basis of the point-charge model [20] enabled us to determine the steric arrangements of the complex species formed. For the calculations, we used the partial quadrupole splitting (pqs) values of the different functional groups (Table 1) that have already

Table 1  
Partial quadrupole splitting (pqs) values used for  $|\Delta|$  calculations ( $\text{mm s}^{-1}$ )

Donor atom or group	Structure			
	tet <sup>a</sup>	tba <sup>a</sup>	tbe <sup>a</sup>	oct <sup>a</sup>
–Me	–1.37	–0.94	–1.13	–1.03
$\text{OH}^-$	–0.20	–0.13	0.02	–0.14
$\text{H}_2\text{O}$	0.43	0.18	0.27	0.09 <sup>b</sup>
$\text{S}^-$	–0.49	–0.60	–0.60	–0.56
$-\text{COO}^-$ (monodentate)	–0.15	–0.10	0.06	–0.11
$-\text{COO}^-$ (bidentate)	0.11	0.08	0.29	–0.08
$-\text{C}=\text{O}$	0.24	0.16	0.41	0.18
N (peptide)	–0.56	–0.37	–0.30	–0.41

Data obtained from Refs. [21–25] and calculated from these for the missing values.

<sup>a</sup> tet, tba, tbe and oct indicate tetrahedral, axial trigonal bipyramidal, equatorial trigonal bipyramidal and octahedral arrangements, respectively.

<sup>b</sup> See text.

been published [21–25]. The pqs value for water–oxygen in an octahedral structure was derived from Mössbauer measurements performed for the  $\text{Me}_2\text{Sn}(\text{IV})$  aquocation in four different systems in the glassy state. For the calculations, the value  $([\text{H}_2\text{O}] - [\text{Cl}])^{\text{oct}} = 0.09$   $\text{mm s}^{-1}$  was used instead of 0.20  $\text{mm s}^{-1}$  [22].

#### 2.6. Biological materials

Adult specimens of *C. intestinalis* (Ascidacea, Urchordata) were collected from the Gulf of Palermo and Marsala, and identified according to Berrill [26]. Male and female gametes were removed from the gonoducts of dissected animals and transferred onto Syracuse dishes. The eggs were reared in Millipore-filtered seawater while the sperms were diluted before insemination to a final suspension of ca. 0.1% v/v.

Soon after fertilization, the eggs were incubated in the presence of light, in separate solutions, at different concentrations and for different exposure times, with free captopril, or with  $\text{Me}_2\text{Sn}(\text{cap})$ ,  $\text{Et}_2\text{Sn}(\text{cap})$ , *n*- $\text{Bu}_2\text{Sn}(\text{cap})$ , *t*- $\text{Bu}_2\text{Sn}(\text{cap})$  or DET (diethyltin dichloride) (positive control), or in simple seawater (negative control).

Five experiments were performed. The eggs were incubated in the organotin(IV)-containing solutions at the 8–16–32-blastomere stages. For each experiment, some of the eggs were transferred to the dialkyltin(IV) (0.5% DMSO) derivative solutions and allowed to develop until the remainder, used as controls, were swimming larvae.

The embryos treated with 0.5% DMSO solution served as controls. Observations were made under a light microscope. The embryos developed into larvae.

All the experiments were performed at 295 K and the pH of the solutions obtained was controlled and

maintained at the normal pH of seawater (7.76–7.78). In vivo observations were made with a Leitz Diaplan microscope and photographs were taken on Kodak  $T_{\max}$  film.

### 3. Results and discussion

#### 3.1. pH-metric measurements

The hydrolysis of  $\text{Me}_2\text{Sn(IV)}^{2+}$  has been investigated in different media by several authors and the results are compiled in [27]. We earlier performed potentiometric titrations to obtain data at an ionic strength of  $0.1 \text{ mol dm}^{-3}$  ( $\text{NaClO}_4$ ) [28] and detected the formation of species with the same composition and similar stability to those reported by Arena et al. [29]. The observed species and overall stability constants are shown in the head of Table 2. Introduction of other polynuclear hydroxo complexes into the species matrix did not improve the fitting. The ligand undergoes two deprotonation steps up to pH 11.5, attributed to the  $-\text{COOH}$  and  $-\text{SH}$  groups of the ligand, with  $pK$  3.52 and 9.88, respectively, as presented in Table 2.

In the applied concentration range, no precipitation was observed in the presence of  $\text{Me}_2\text{Sn(IV)}^{2+}$ . The best fit was obtained for the model shown in Table 2. The protonation and complex formation constants calculated from the pH-metric titrations, together with some derived data, are also collected here. The species distribution curves depicted in Fig. 2 demonstrate that mostly complexes with ligand-to-metal ratio of 1:1 were formed. The only except ion is the species  $\text{ML}_2$  formed in detectable amount above pH 4 when a ligand excess was used. There was no evidence of the presence of polynuclear species in solution. The 1:1 species formed at different pH values were found to be in different protonation states.

All deprotonation processes resulting in complex molecules take place in the acidic pH range (Fig. 2).

Table 2  
Protonation and  $\text{Me}_2\text{Sn(IV)}$  complex formation constants of captopril

$\log \beta(\text{LH}_2)$	13.40(1)
$\log \beta(\text{LH})$	9.88(1)
$\log \beta(\text{MLH})$	13.35(3)
$\log \beta(\text{ML})$	10.46(1)
$\log \beta(\text{MLH}_{-1})$	4.99(1)
$\log \beta(\text{ML}_2)$	17.18(2)
$pK(\text{LH}_2)$	3.52
$pK(\text{LH})$	9.88
$pK(\text{MLH})$	2.89
$pK(\text{ML})$	5.47

The hydrolysis constants for  $\text{Me}_2\text{Sn(H}_2\text{O)}_n(\text{IV})^{2+}$  ( $=\text{M}$ ) are:  $\log \beta(\text{MH}_{-1})$ :  $-3.12$ ;  $\log \beta(\text{MH}_{-2})$ :  $-8.33$ ;  $\log \beta(\text{MH}_{-3})$ :  $-19.33$ ;  $\log \beta(\text{M}_2\text{H}_{-2})$ :  $-4.83$ ;  $\log \beta(\text{M}_2\text{H}_{-3})$ :  $-9.69$ .

Already at the starting pH, a complex with the composition  $\text{MLH}$  is present. This species is formed by the coordination of a single deprotonated ligand, most likely on its  $-\text{COOH}$  group.  $\text{ML}$  is formed with the deprotonation of  $\text{MLH}$ , which corresponds to the deprotonation of the thiol group on the ligand. The  $pK$  of this process (defined as  $\log \beta(\text{MLH}) - \log \beta(\text{ML})$ ) is 7 units lower than  $pK(\text{LH})$  due to the metal-promoted deprotonation and coordination of the thiol group. Our suggestion about the donor groups in  $\text{ML}$  is confirmed by the X-ray structure of the complex  $\text{Me}_2\text{Sn}(\text{cap})$  crystallized from aqueous solution in this pH range [16]. It was found that in this complex the captopril is coordinated to the central  $\{\text{Sn}\}$  atom by its  $-\text{COO}^-$ ,  $-\text{S}^-$  and amide  $-\text{C}=\text{O}$  groups, forming  $\text{tbp}$  geometry around the metal ion.

In the next step, two processes take place, resulting in complex molecules. One can be assigned to the formation of  $\text{MLH}_{-1}$ , with displacement of the  $-\text{COO}^-$  group from the coordination sphere by  $\text{OH}^-$ , while the other one,  $\text{ML}_2$  (depending on the ligand-to-metal ratio) is most probably formed through the substitution of the same group by the thiolate group of another ligand.

#### 3.2. Mass spectrometric measurements

Mass spectrometry can be a useful tool in the investigation of peptides and their complexes [30]. Captopril and its metal complexes in solution have already been studied by this technique [31]. Owing to the multiisotopic nature of tin, the signals of metal-containing species can easily be recognized in each spectrum. Additionally, the charge on the tin-containing species and the number of  $\{\text{Sn}\}$  atoms within a molecule ion can be determined from a comparison of the simulated isotope distribution pattern with that found.

Mass spectra were recorded at two characteristic pH values, 4.3 and 8.2, where the Mössbauer measurements were also performed. In the present case, only a set of singly charged ions were observed. Parameters of the characteristic peaks occurred in the spectra are presented in Table 3.

The species distribution curve indicates that at pH 4.3 the main species in solution is the complex  $\text{ML}$ . In accordance, in the mass spectrum of  $\text{M:L} = 1:1$  in  $[\text{M}] = 1 \text{ mmol dm}^{-3}$  solution the base peak can be assigned to the  $(\text{ML} + \text{H})^+$  singly charged cation (Table 3), which is also confirmed by the isotopic pattern characteristic of compounds containing one  $\{\text{Sn}\}$  atom (Fig. 3). Besides the peak corresponding to the free ligand  $(\text{LH}_2 + \text{H})^+$ , another low-intensity line can be observed at  $m/z = 729.0$ , due to the dimeric ion  $(\text{M}_2\text{L}_2 + \text{H})^+$ . This species is formed in a very low amount in the gaseous phase, but cannot be detected by evaluation of the titration data.

In order to detect both  $\text{MLH}_{-1}$  and  $\text{ML}_2$  present in solution at pH 8.2, two mass spectra were recorded in

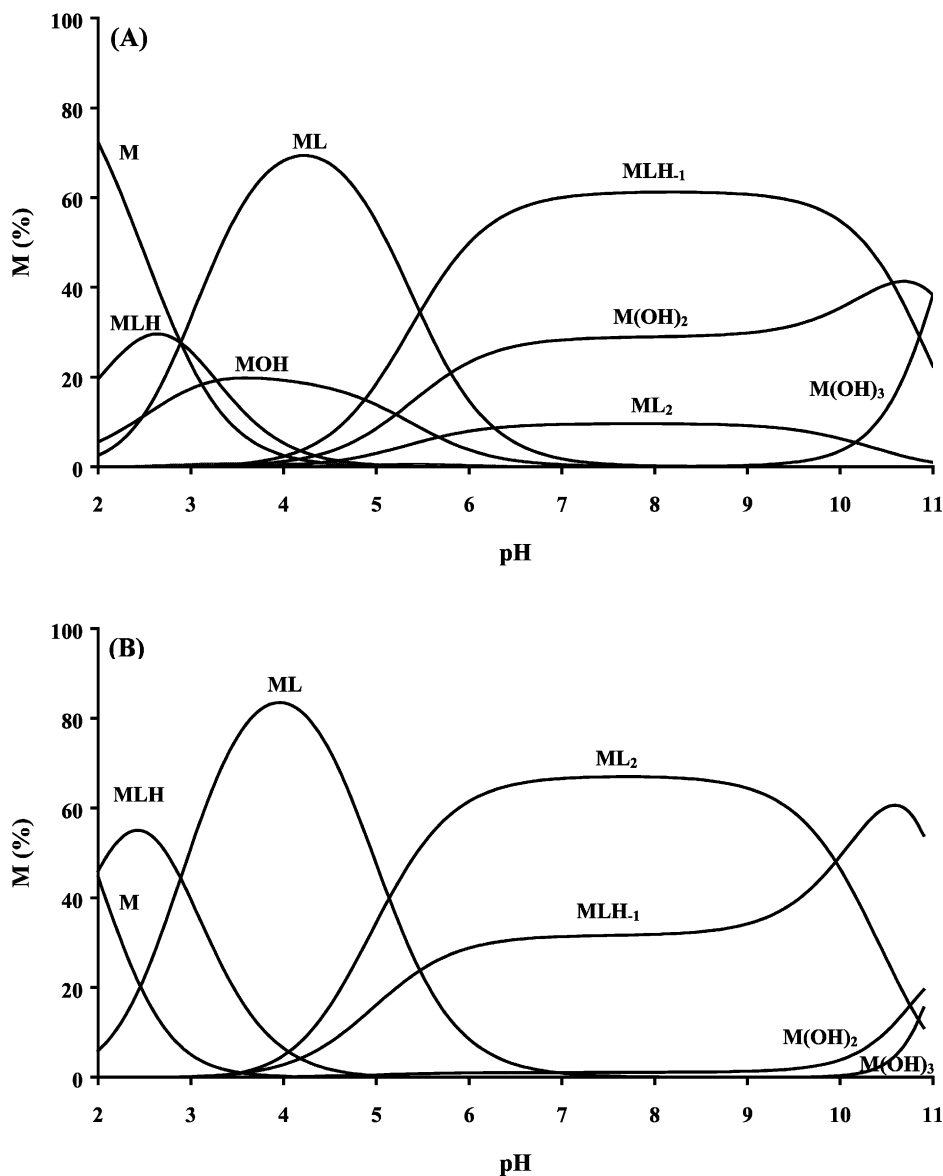


Fig. 2. Species distribution diagrams for the 1:1 (A) and 1:10 (B)  $\text{Me}_2\text{Sn(IV)-captopril}$  system,  $[\text{Me}_2\text{Sn(IV)}^{2+}] = 0.005 \text{ mol dm}^{-3}$ .

the positive ion mode, using ligand-to-metal ratios of 1:1 and 10:1. The neutral hydrolysis species  $\text{Me}_2\text{S-}$

$n(\text{OH})_2(\text{H}_2\text{O})_n$ , represented in the species matrix as  $\text{M}(\text{OH})_2$ , was not expected to appear in the spectra.

Table 3  
 $m/z$  value and relative abundance (in parentheses) of the characteristic peaks in the mass spectra

pH	L:M used	$(\text{L}+3\text{H})^+$	$(\text{ML}+\text{H})^+$	$(2\text{L}+5\text{H})^+$	$(2\text{ML}+\text{H})^+$
4.3	1:1	217.8 (65.5)	365.9 (100)	433.1 (9.0)	729.0 (11.0)
8.2	1:1	217.8 (45.0)	365.9 (100)	433.1 (4.2)	729.1 (8.2)
8.2	10:1	217.9 (100)	366.0 (46.3)	433.3 (4.0)	729.2 (3.0)
		$(\text{L}+\text{H})^-$	$(\text{ML}+\text{Cl})^-$	$(2\text{L}+3\text{H})^-$	$(\text{ML}_2+\text{H})^-$
8.2	10:1	215.7 (100)	399.9 (24.5)	430.9 (25.0)	581.0 (14.6)



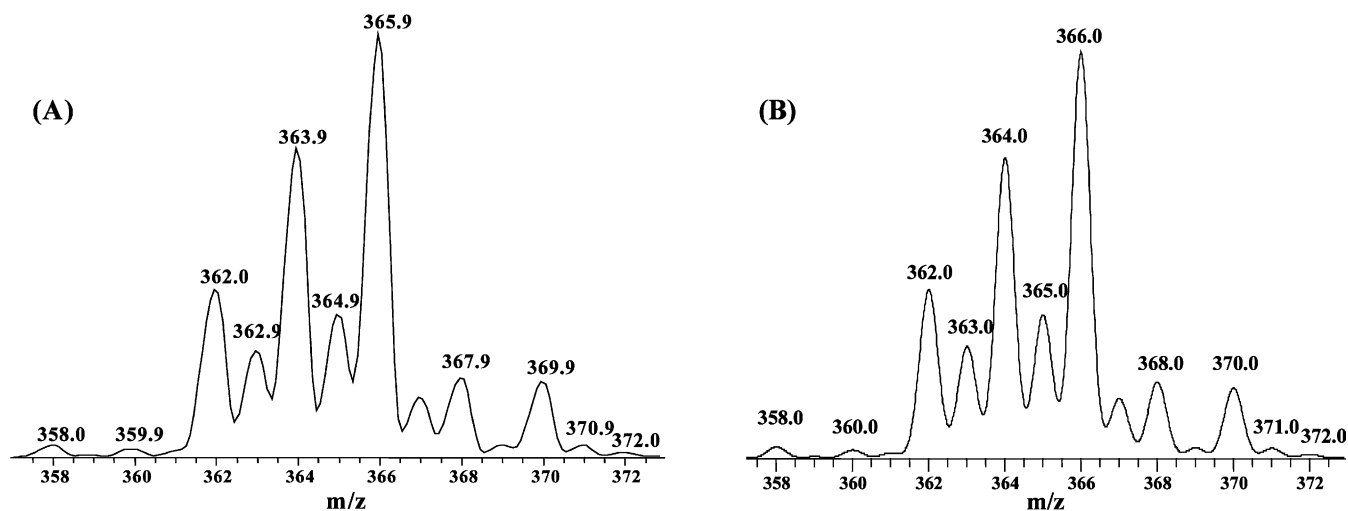


Fig. 3. Measured (A) and simulated (B) special tin isotopic pattern for the monomeric complex ion  $(ML+H)^+$ .

There was no significant difference between the spectrum recorded at pH 8.2 and that recorded at pH 4.3, except for the position of the base peak of the solution prepared with a metal-to-ligand ratio of 10:1, which was at 217.9 due to the ligand excess. The peak corresponding to  $(ML_2+3H)^+$  was present in the spectrum of the 10:1 solution, but its intensity was very low, possibly because of the prevented uptake of the third proton.

The spectrum of the 10:1 solution at pH 8.3 was recorded in the negative ion mode too, to confirm the presence of the species  $ML_2$ . Due to the ligand excess, the base peak was  $(L+H)^-$  at  $m/z$  215.7. Besides the peaks of  $(ML+Cl)^-$  and  $(2L+3H)^-$ , the peak at 581.0, attributed to  $(ML_2+H)^-$ , was also present in the spectrum. Chloride ion came from the starting material,  $Me_2SnCl_2$ . The isotopic pattern of  $(ML+Cl)^-$  and  $(ML_2+H)^-$  as compared to the calculated one strongly supported our suggestion.

### 3.3. NMR studies

Lockhart and Manders studied the correlation of  $^2J(Sn-^1H)$  and the C–Sn–C angle in 25 methyltin(IV) compounds [32]. A plot of these data reveals that  $\theta$  and  $^2J(Sn-^1H)$  are related by the curve described by Eq. (4); the data for most of the compounds lie within  $4^\circ$  of this empirical line.

$$\theta(^{\circ}) = 0.0161|^2J(Sn-^1H)|^2 - 1.32|^2J(Sn-^1H)| + 133.4 \quad (4)$$

The two-bond coupling  $^2J(Sn-^1H)$  of the  $Me_2Sn(IV)^{2+}$  complexes can be determined via the  $^1H$ -NMR spectra of these compounds, if the ligand has no signal in the range of the Me protons. The signal of the methyl group of captopril in aqueous solution falls in the range 1.0–1.2 ppm, which allows determination of the coupling  $^2J(Sn-^1H)$ . These values provide

information on the average C–Sn–C bond angle of the compounds in a sample and indirectly on the possible coordination numbers and geometry around the  $\{Sn\}$  atom. The coupling constants  $^2J(Sn-^1H)$  for the  $Me_2Sn(IV)^{2+}$ –captopril system, together with the calculated C–Sn–C bond angles, are collected in Table 4.

In order to obtain high-quality spectra within a normal detection time interval, measurements were performed in  $[M] = 0.01 \text{ mol dm}^{-3}$  solutions. At this concentration in the pH range 3–6.5, a precipitate is formed in solution. Samples were therefore taken for measurements from the supernatant.

At pH 1.20 the  $^1H$ -NMR Me proton signal is very narrow, suggesting one tin-containing species present in solution. The calculated C–Sn–C bond angle is very close to  $180^\circ$ , which is in good agreement with that found for *trans* octahedral  $Me_2Sn(H_2O)_4^{2+}$  by Möss-

Table 4

$^1H$ -NMR parameters and couplings  $^2J(Sn-^1H)$  of the Me protons in the 1:1 solutions of  $Me_2Sn(IV)^{2+}$ :captopril system,  $[Me_2Sn(IV)^{2+}] = 0.01 \text{ mol dm}^{-3}$ ,  $I = 0.1 \text{ mol dm}^{-3}$  ( $NaClO_4$ ) and the calculated C–Sn–C angles in the pH range 1–11

pH	$\delta$ (ppm)	Line-width <sup>a</sup> (Hz)	$^2J(^1H-(^{119}Sn))$ (Hz)	$\theta$ (C–Sn–C) <sub>calc</sub> <sup>b</sup> ( $^\circ$ )
1.20	0.95	1.79	106.8	176.1
1.96	0.93	2.68	101.9	166.1
2.70	0.91	2.12	92.2	148.6
3.19	0.90	1.60	88.5 <sup>c</sup>	142.7
6.12	0.77	19.70	– <sup>c</sup>	–
7.27	0.75	10.98	78	128
8.30	0.77	2.78	75.7	125.7
9.28	0.76	1.84	76.3	126.4
10.46	0.72	1.30	78.4	128.9

<sup>a</sup> Line-width: the half-line-width of the methyl protons in  $Me_2Sn(IV)^{2+}$ .

<sup>b</sup> Calculated via Eq. (4) in [32].

<sup>c</sup> Sampling from the supernatant of the precipitated solution.

bauer spectroscopic measurements [33]. On increase of the pH to 3.19, the Me proton signal shifts to higher fields, similarly as found for a solution of  $\text{Me}_2\text{Sn(IV)}^{2+}$  [34], but to a lesser degree, showing the participation of the metal ion in interactions other than hydrolysis, as well, which is supported by the broadened signal. At the same time, the calculated average C–Sn–C angle decreases, demonstrating the presence of a species with Me groups not in the *trans* position. On the basis of the calculated value and our earlier findings concerning the structure of the neutral solid complex [16], in the complex molecules formed in solution a *tbp* arrangement is presumed, with *eq* Me groups.

In the relatively concentrated solution, most probably oligomeric species are present. Hence, the Me proton signal in the spectrum recorded at pH 6.12 on the solution above the partially dissolved precipitate was much too broadened to find satellites for determination of the coupling constant. Nevertheless, a further upfield shift of this signal can be observed in the spectrum. From the physiological pH, the coupling  $^2J(\text{Sn}-^1\text{H})$  does not change dramatically, and the calculated C–Sn–C angles are close to  $120^\circ$ , suggesting the presence of  $\text{Me}_2\text{Sn(IV)}$  compounds in solution with *eq* *tbp* Me groups. This is in line with our earlier findings on the present hydrolysis species [34]. The chemical shift of the Me proton signal does not undergo a significant change with increasing pH; it is at around 0.75 ppm. This is different from the situation for the solution of  $\text{Me}_2\text{Sn(IV)}^{2+}$ , in which the signal of the Me protons is shifted to 0.64 ppm in the pH range 7.4–10.0, and further upfield on increase of the pH [34]. The difference probably stems from the presence of  $\text{ML}_2$ , as shown by the pH-metric measurements.

Since  $^1J(^{13}\text{C}-^{119}\text{Sn})$  coupling can also be used for determination the C–Sn–C bond angle [35],  $^{13}\text{C}$ - and  $^{119}\text{Sn}$ -NMR measurements were performed in 1:2 solution of  $\text{Me}_2\text{Sn(IV)}^{2+}$ -captopril at pH 9. In order to obtain valuable spectra, concentration of the metal ion was increased up to 0.025 M. Species distribution curve extrapolated to this concentration shows the presence of two  $\text{Me}_2\text{Sn(IV)}^{2+}$ -containing species ( $\text{ML}_2$  ( $\approx 63\%$ ) and  $\text{MLH}_{-1}$  ( $\approx 36\%$ )). Due to the ligand, bound  $\text{OH}^-$  and  $\text{H}_2\text{O}$  exchange on  $\text{Me}_2\text{Sn(IV)}^{2+}$ , the  $\text{CH}_3(\text{Sn})$ -signal is broadened and  $^1J(^{13}\text{C}-^{119}\text{Sn})$  coupling cannot be determined with sufficient certainty from the spectrum. The same reason leads to a non-informative  $^{119}\text{Sn}$ -NMR spectrum. Owing to the formation of precipitation in the pH range of 2–6, concentration of  $\text{Me}_2\text{Sn(IV)}^{2+}$  and the ligand cannot be increased sufficiently for  $^{13}\text{C}$ - and  $^{119}\text{Sn}$ -NMR measurements.

### 3.4. Sn Mössbauer study

Since the information about the coordination sphere around the tin atom in the complexes afforded by the

NMR measurements is limited, Mössbauer measurements in quick-frozen solutions were also performed at two pH values. As several examples have already demonstrated, application of this method for structural studies of complexes formed in aqueous solution can be a powerful tool (e.g. [9,14,15]). In this particular case, taking into account the concentration limit for  $\text{Me}_2\text{Sn(IV)}^{2+}$  determined by the precipitation occurs at low pH, the sufficient detection time increases up to several days. In spite of the long time required by the measurements, the Mössbauer spectra obtained are not of such good quality as the spectra of solid complexes, and the parameters obtained from them may involve larger errors than usual.

For Mössbauer measurements, two pH values, 4.3 and 8.2, were chosen in solution at a metal-to-ligand ratio of 1:1. As expected from the results of the pH-metric titrations, the spectra obtained were not symmetric doublets; thus, both of them were decomposed into two. The integrals of the doublets compared to the distribution curve allow the measured  $|\Delta|$  values to be ascribed to the appropriate species. The pqs calculations were performed only for the main compound present at the given pH.

At pH 4.3, the doublet with larger integral is attributed to the complex  $\text{ML}$ , with  $|\Delta_{\text{calc}}| = 3.02 \text{ mm s}^{-1}$ . The coordination of  $-\text{S}^-$  and  $-\text{COO}^-$  in  $\text{ML}$  has been revealed by pH-metry, and only monomeric complexes were found on the evaluation of concentration-dependent titrations. Since coordination of the amide  $-\text{C}=\text{O}$  group cannot be proved or excluded by pH-metry, this and coordinating  $\text{H}_2\text{O}$  molecules (one or two) were also taken into account in the pqs calculations. The best agreement between the measured and calculated data was found for a *tbp* arrangement in which the thiolate and carboxylate groups are coordinated in *eq* and *ax* positions, respectively. One  $\text{H}_2\text{O}$  molecule coordinates axially and the Me groups, in agreement with the  $^1\text{H}$ -NMR results, equatorially. The experimental  $|\Delta|$  is very close to that obtained for the polymeric solid complex  $\text{Me}_2\text{Sn}(\text{cap})$  ( $2.93 \text{ mm s}^{-1}$ ), in which the *tbp* geometry around the tin involves an *eq* thiolate and an *ax* amide  $-\text{C}=\text{O}$  of one ligand and an *ax* carboxylate of another, while Me groups occupy the remaining *eq* positions.

As can be seen from the species distribution curve (Fig. 2), at pH 8.2 the main species in solution is  $\text{MLH}_{-1}$ . Thus, the value of  $|\Delta_{\text{exp}}| = 2.89 \text{ mm s}^{-1}$  obtained for the doublet with the larger integral area of the decomposed Mössbauer spectrum was attributed to this species. The results of pH-metric titrations and earlier findings [27] indicate that the carboxylate group is not able to protect  $\text{Me}_2\text{Sn(IV)}^{2+}$  from hydrolysis in this pH range: a hydroxide ion displaces it in the coordination sphere. The result of pqs calculations

lend further support to this suggestion: if the contribution of an  $ax$   $\text{OH}^-$  is used in the calculation instead of the contribution of the  $ax$   $-\text{COO}^-$ ,  $|\Delta_{\text{calc}}| = 3.10 \text{ mm s}^{-1}$  is obtained, which is within the acceptable limit of  $0.4 \text{ mm s}^{-1}$  for the difference  $|\Delta_{\text{calc}} - \Delta_{\text{exp}}|$ .

Mössbauer spectrum obtained at pH 8.9, M:L = 1:10 can be decomposed into two doublets. Ratio of the integrals is 1:2, similarly to  $\text{MLH}_{-1}:\text{ML}_2$  at this pH (Fig. 2B). Based on this, parameters of the doublet with the larger integral ( $\delta = 1.28 \text{ mm s}^{-1}$ ,  $|\Delta| = 2.25 \text{ mm s}^{-1}$ ) could be attributed to  $\text{ML}_2$ . Based on pq calculations,  $|\Delta|$  is in the best agreement with the calculated  $2.03 \text{ mm s}^{-1}$  value, which describes a tetrahedral arrangement with double thiolate coordination.

### 3.5. Results of biological tests

In a  $0.01 \text{ mol dm}^{-3}$  or more concentrated solution of  $\text{Me}_2\text{Sn(IV)}^{2+}:\text{captopril} = 1:1$  in the pH range 2.5–5.0 a precipitate is formed. This was characterized by several spectroscopic methods, and also by X-ray crystallography [16]. Three other  $\text{R}_2\text{Sn(IV)}$  ( $\text{R} = \text{Et}$ ,  $n\text{-Bu}$  and  $t\text{-Bu}$ ) complexes of captopril were also synthesized and studied by elemental analysis, FTIR and  $^{119}\text{Sn}$  Mössbauer spectroscopy, as described previously. The solubility of these complexes in water was very low and two of those [ $\text{Et}_2\text{Sn}(\text{cap})$  and  $t\text{-Bu}_2\text{Sn}(\text{cap})$ ] were practically insoluble in all common NMR solvents. This fact limited their further study in solution. Their characterization in the solid state suggested a very similar structure in all cases, i.e. 1:1 polymeric complexes, with thiolate, carboxylate and amide  $-\text{C}=\text{O}$  coordination. In order to evaluate and compare the possible cytotoxicity of the complexes, the development of *C.*

*intestinalis* embryos after treatment with these chemicals was analysed at different concentrations. The results are given in Table 5.

The embryo development seemed to parallel that regularly observed for fertilized eggs of *C. intestinalis* [36]. In fact, the development of these embryos resulted in two to four blastomeres, gastrula and neurula stages after 2, 6 and 7.5 h, respectively. Moreover, after 24 h the embryos were in the swimming larva stage, with a trunk and a tail (Fig. 4). The eggs incubated in the ligand developed normally up to the larval stage at a percentage (70%) identical to that for the controls.

Normal larvae were obtained after treatment with  $\text{Me}_2\text{Sn}(\text{cap})$  or  $\text{Et}_2\text{Sn}(\text{cap})$  at both  $10^{-5}$  and  $10^{-7} \text{ mol dm}^{-3}$ , and also after treatment with DET.

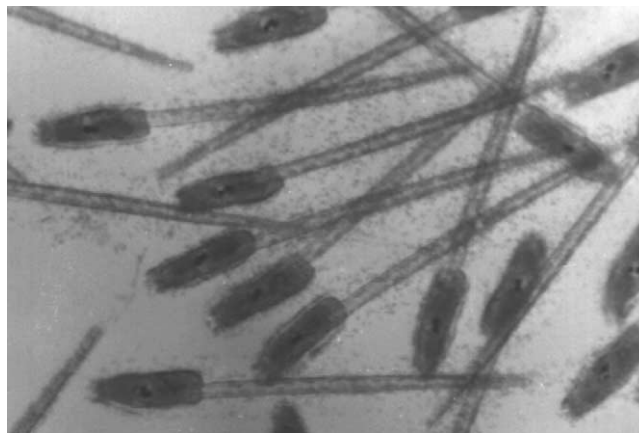


Fig. 4. *C. intestinalis* swimming larvae (magnification  $\times 48$ ).

Table 5

Results of development of fertilized *C. intestinalis* eggs incubated in solutions of  $\text{R}_2\text{Sn}(\text{cap})$  from the 8-16-32-cell stage

Compound	Concentration ( $\text{mol dm}^{-3}$ )	Development stages			
		Uncleaved eggs	Anomalous embryos	Anomalous larvae	Normal larvae
Captopril	$10^{-5}$	10	15	5	70
	$10^{-7}$	10	15	5	70
DET	$10^{-5}$	10	15	5	70
	$10^{-7}$	10	15	5	70
$\text{Me}_2\text{Sn}(\text{cap})$	$10^{-5}$	10	15	5	70
	$10^{-7}$	10	15	5	70
$\text{Et}_2\text{Sn}(\text{cap})$	$10^{-5}$	10	15	5	70
	$10^{-7}$	10	15	5	70
$n\text{-Bu}_2\text{Sn}(\text{cap})$	$10^{-5}$	10	90		
	$10^{-7}$	10	80	5	5
$t\text{-Bu}_2\text{Sn}(\text{cap})$	$10^{-5}$	10	90		
	$10^{-7}$	10	80	5	5

The data relate to five experiments and show the percentages of developed or arrested eggs. The controls developed 70% swimming larvae. All the experiments were performed at 295 K and pH 7.76–7.78.



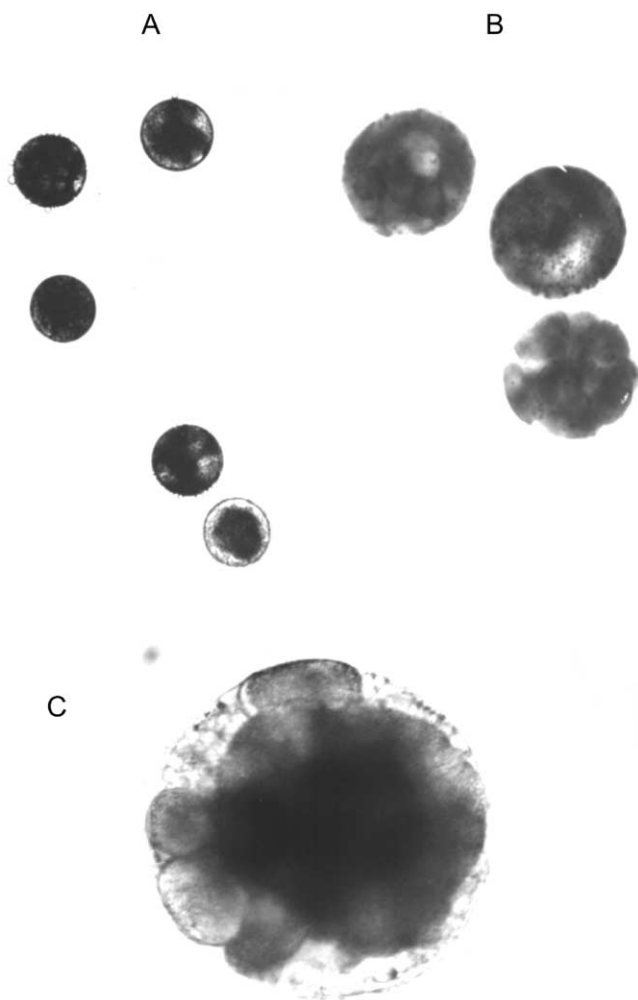


Fig. 5. Anomalous embryos of *C. intestinalis* incubated in  $10^{-5}$  mol dm $^{-3}$  *n*-Bu $_2$ Sn(cap) solution. (A) In some embryos where the test and follicular cells are detached, hyaline protrusions are visible. (B, C) Inside, the blastomeres are arranged in a chaotic pattern (magnification, (A)  $\times 58$ ; (B)  $\times 144$ ; (C)  $\times 360$ ).

Although at a very low percentage, normal larvae were obtained after treatment with *n*-Bu $_2$ Sn(cap) or *t*-Bu $_2$ Sn(cap) at  $10^{-7}$  mol dm $^{-3}$ . *n*-Bu $_2$ Sn(cap) at  $10^{-5}$  mol dm $^{-3}$  inhibited cleavage of the eggs in the 8-16-32-blastomere stages strongly anomalously (Fig. 5). *t*-Bu $_2$ Sn(cap) at  $10^{-5}$  mol dm $^{-3}$  blocked the development when embryos reached an advanced stage, giving rise to anomalous embryonic masses (Fig. 6). The main results obtained were as follows:

- 1) The ligand does not affect the embryonic development of *C. intestinalis* significantly.
- 2) Me $_2$ Sn(cap) and Et $_2$ Sn(cap) do not affect the embryonic development; *n*-Bu $_2$ Sn(cap) and *t*-Bu $_2$ Sn(cap) exert toxic activity on *C. intestinalis* embryos in the early stages of development. This toxicity is concentration-dependent and is related to the lipophilic properties of the complexes.

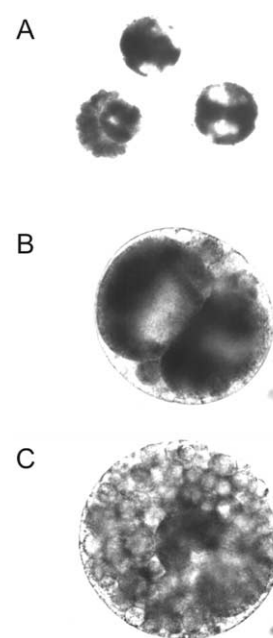


Fig. 6. Anomalous embryos of *C. intestinalis* incubated in  $10^{-5}$  mol dm $^{-3}$  *t*-Bu $_2$ Sn(cap) solution. (A) The blastomeres are of different sizes and are blocked. (B, C) They present an anomalous distribution of plasms and are arranged in a chaotic pattern, with a non-uniform distribution of hyaline and dark areas in the different parts of embryo (magnification, (A)  $\times 72$ ; (B, C)  $\times 180$ ).

#### 4. Conclusions

Captopril, an ACE inhibitor, is not only interesting from medicinal and biological aspects; it is also a versatile ligand, with four potential donor groups for the formation of coordination compounds. Moreover, it is a Cys-Pro-like pseudo-dipeptide. These facts have placed it in the focus of coordination chemistry research, and its interactions towards most of the transition metal ions have been described in detail. In the first study of organometallic compounds of captopril [16], four R $_2$ Sn(IV) (R = Me, Et, *n*-Bu and *t*-Bu) complexes of captopril were synthesized and characterized by means of FtIR, Raman and  $^{119}$ Sn-NMR spectroscopy and electrospray mass spectrometry. Additionally, the structure of Me $_2$ Sn(cap) was determined by single-crystal X-ray diffraction method. Comparison of the results obtained by the different methods for the individual compounds showed that their structures are very similar, differing only in the degree of distortion of the bond angles. Each complex adopts a linear polymeric structure, with a *tbp* arrangement around the tin atom. The metal centres are linked by a chelate-type coordination of the thiolate group and the amide  $-C=O$  of one ligand in the *eq-ax* position and *ax* coordination of a carboxylate group of another [16].

Since Me $_2$ Sn(IV) $^{2+}$  and captopril are soluble in water, to acquire a better insight into the coordination processes that take place in solution, we extended these

studies to the interactions in aqueous solution in the pH range 2–11. In this work, the equilibrium behaviour and possible structures of the complexes formed under these conditions are discussed in detail. Evaluation of the pH-metric titration data revealed that in the acidic pH range monomeric complexes are formed with a metal-to-ligand ratio of 1:1, which differ from each other only in the protonation state. In the first step, the carboxylate group of captopril is deprotonated. The neutral complex ML is then formed through the deprotonation and coordination of the thiol group. This pH range is that in which the solid complex  $\text{Me}_2\text{Sn}(\text{cap})$  precipitated from more concentrated solutions, which makes a comparison of the structures of the two complexes interesting. These are very similar as far as the geometry around the central tin atom is concerned. The only difference is that in the solid complex the amide  $-\text{C}=\text{O}$  is coordinated in one of the *ax* positions, while in ML a  $\text{H}_2\text{O}$  molecule is found there.

On increase of the pH, two new processes take place, resulting in complex molecules, each involving displacement of the carboxylate group from the coordination sphere. In  $\text{MLH}_{-1}$  a hydroxide ion completes the structure to *tbp*. In  $\text{ML}_2$  thiolate groups of two ligands coordinates to  $\text{Me}_2\text{Sn}(\text{IV})^{2+}$  forming tetrahedral structure.

Among the methods used for the structural studies of the complexes formed in aqueous solution  $^{119}\text{Sn}$  Mössbauer spectroscopy proved to be the only efficient one.

To add to the results that we have obtained so far, the cytotoxicity of the four  $\text{R}_2\text{Sn}(\text{IV})$  complexes was also investigated. Biological activity tests of the  $\text{R}_2\text{Sn}(\text{IV})$  complexes under study demonstrated that *n*- $\text{Bu}_2\text{Sn}(\text{cap})$  or *t*- $\text{Bu}_2\text{Sn}(\text{cap})$  exerts toxic activity towards the embryos of *C. intestinalis*, while the ligand itself does not affect the development of the embryos to any significant extent;  $\text{Me}_2\text{Sn}(\text{cap})$  and  $\text{Et}_2\text{Sn}(\text{cap})$  produced normal swimming larvae.

The mechanism of action of the tested compounds is still unknown, but literature data on the highly toxic tributyltin(IV)<sup>+</sup> indicate that this chemical alters the intracellular  $\text{Ca}^{2+}$  homeostasis through inhibition of the membrane  $\text{Ca}^{2+}$ -ATPase, which activates several processes, causing first microfilament and microtubule disassembly [37] or chromosomal disorders, with alteration of the cytoplasmic organelles and cell metabolism [38–41].

### Acknowledgements

Financial support by the Hungarian Research Foundation (OTKA T032067 and T029554), the Ministero dell'Istruzione, dell'Università e della Ricerca (M.I.U.R., Rome); the Università di Palermo, Palermo; the Hungarian–Italian Intergovernmental Scientific and

Technological Programme (I-4/95) and FKFP (015/1999); the University of Camerino and the Carima Foundation is gratefully acknowledged. One sample of the ligand was a generous gift from Dr P. Tömpe (EGIS Pharmaceutical Company, Hungary).

### References

- [1] J.E.F. Reynolds (Ed.), Martindale, The Extra Pharmacopoeia, 31st ed., The Pharmaceutical Press, London, 1996, pp. 821 and 838.
- [2] R.C. Heel, R.N. Brodgen, T.M. Speight, G.S. Avery, *Drugs* 20 (1980) 409.
- [3] F.A. Catalanotto, *Am. J. Clin. Nutr.* 31 (1978) 1098.
- [4] M.A. Hughes, G.L. Smith, D.R. Williams, *Inorg. Chim. Acta* 107 (1985) 247.
- [5] G.L. Christie, M.A. Hughes, S.B. Rees, D.R. Williams, *Inorg. Chim. Acta* 151 (1988) 215.
- [6] P.A.M. Williams, E.G. Ferrer, E.J. Baran, *J. Coord. Chem.* 42 (1997) 261.
- [7] H. Kőszegi-Szalai, T.L. Paál, L. Barcza, *Z. Phys. Chem.* 214 (2000) 45.
- [8] T. Jovanovič, B. Stanovič, Z. Korčanak, *J. Pharm. Biomed. Anal.* 13 (1995) 213.
- [9] R. Barbieri, M.T. Musmeci, *J. Inorg. Biochem.* 32 (1988) 89.
- [10] M.T. Musmeci, G. Madonia, M.T. Lo Giudice, A. Silvestri, G. Ruisi, R. Barbieri, *Appl. Organomet. Chem.* 6 (1992) 127.
- [11] F. Huber, G. Roge, L. Carl, G. Atassi, F. Spreafico, S. Filippeschi, R. Barbieri, A. Silvestri, E. Rivarola, G. Ruisi, F. Di Bianca, G. Alonzo, *J. Chem. Soc. Dalton Trans.* (1985) 523.
- [12] R. Barbieri, A. Silvestri, S. Filippeschi, M. Magistrelli, F. Huber, *Inorg. Chim. Acta* 177 (1990) 141.
- [13] M.J. Hynes, M. O'Dowd, *J. Chem. Soc. Dalton Trans.* (1987) 563.
- [14] F. Capolongo, A.M. Giuliani, M. Giomini, U. Russo, *J. Inorg. Biochem.* 49 (1993) 275.
- [15] N. Buzás, T. Gajda, E. Kuzmann, L. Nagy, A. Vértés, K. Burger, *Main Group Met. Chem.* 18 (1995) 641.
- [16] H. Jankovics, C. Pettinari, F. Marchetti, E. Kamu, L. Nagy, S. Troyanov, T. Fiore, L. Pellerito, *J. Inorg. Biochem.*, submitted for publication (2003).
- [17] F.J.C. Rossotti, H. Rossotti, *The Determination of Stability Constants*, McGraw-Hill Book Co, New York, 1961, p. 149.
- [18] E. Högföldt, *Stability Constants of Metal-Ion Complexes (Part A)*, Pergamon, New York, 1982, p. 32.
- [19] L. Zékány, I. Nagypál, G. Peintler, *PSEQUAD for Chemical Equilibria*, Technical Software Distributors, Baltimore, Maryland, 1991.
- [20] G.M. Bancroft, R.H. Platt, *Adv. Inorg. Chem. Radiochem.* 15 (1972) 59.
- [21] M.G. Clark, A.G. Maddock, R.H. Platt, *J. Chem. Soc. Dalton Trans.* (1972) 281.
- [22] G.M. Bancroft, V.G. Kumar Das, T.K. Sham, M.G. Clark, *J. Chem. Soc. Dalton Trans.* (1976) 643.
- [23] L.A. Asanov, V.N. Ionov, V.M. Attiya, A.B. Permin, V.S. Petrosyan, *J. Organomet. Chem.* 144 (1978) 39.
- [24] R. Barbieri, L. Pellerito, F. Huber, *Inorg. Chim. Acta Lett.* 30 (1978) L321.
- [25] R. Barbieri, *Möss. Eff. Res. Data J.* 6 (1983) 69.
- [26] N.J. Berrill, *The Tunicata*, Ray Society, London, 1950, pp. 1–354.
- [27] L. Pellerito, L. Nagy, *Coord. Chem. Rev.* 224 (2002) 111.

- [28] N. Buzás, T. Gajda, L. Nagy, E. Kuzmann, A. Vértes, K. Burger, *Inorg. Chim. Acta* 274 (1998) 167.
- [29] G. Arena, R. Purrello, E. Rizzarelli, E. Gianguzza, L. Pellerito, *J. Chem. Soc. Dalton Trans.* (1989) 773.
- [30] H. Li, K.W.M. Siu, R. Guevremont, J.C.Y. Le Blanc, *J. Am. Soc. Mass Spectrom.* 8 (1997) 781.
- [31] M.T. Fernandez, M.M. Silva, L. Mira, M.H. Florêncio, A. Gill, K.R. Jennings, *J. Inorg. Biochem.* 71 (1998) 93.
- [32] T.P. Lockhart, W.F. Manders, *Inorg. Chem.* 25 (1986) 892.
- [33] R. Barbieri, A. Silvestri, *Inorg. Chim. Acta* 188 (1991) 95.
- [34] H. Jankovics, L. Nagy, N. Buzás, L. Pellerito, R. Barbieri, *J. Inorg. Biochem.* 92 (2002) 55.
- [35] T.P. Lockhart, W.F. Manders, J.J. Zuckerman, *J. Am. Chem. Soc.* 107 (1985) 4546.
- [36] W.R. Jeffery, B.Y. Swalla, Tunicates, in: S.F. Gilbert, A.M. Raunio (Eds.), *Embryology: Constructing the Organism* (Ch. 17), Sinauer Associates, Sunderland, USA, 1997, p. 331.
- [37] F. Cima, L. Ballarin, G. Bressa, G. Martinucci, P. Burighel, Toxicity of organotin compounds on embryos of a marine invertebrate (*Styela plicata*; Tunicata), *Ecotoxicol. Environ. Saf.* 35 (1996) 174.
- [38] C. Mansueto, L. Pellerito, M.A. Girasolo, *Acta Embryol. Exper. N.S.* 6 (1989) 237.
- [39] C. Mansueto, M. Gianguzza, G. Dolcemascio, L. Pellerito, *Appl. Organomet. Chem.* 7 (1993) 391.
- [40] C. Mansueto, E. Puccia, F. Maggio, R. Di Stefano, T. Fiore, C. Pellerito, F. Triolo, L. Pellerito, *Appl. Organomet. Chem.* 14 (2000) 229.
- [41] M. Marinovich, B. Viviani, C.L. Galli, *Toxicol. Lett.* 52 (1990) 311.